

Electronic Supplementary Information

Interrogating Biomineralization One Amino Acid at a Time: Amplification of Mutational Effects in Protein-Aided Titania Morphogenesis through Reaction Diffusion Control

Karthik Pushpavanam, Brittney Hellner and François Baneyx*

Department of Chemical Engineering, University of Washington, Seattle, WA, 98195

Table S1. Peptides, proteins and organisms used in the mineralization of TiO₂. All studies used TiBALDH as a precursor except for reference 2, which relied on titanium isopropoxide. Titania precipitates were obtained by bulk mixing of the reagents except for references (7) and (9) in which a “layer-by-layer” processing was used. The morphology and crystallinity of the precipitates is indicated. The table is not exhaustive.

PEPTIDE	PARTICLE MORPHOLOGY	CRYSTALLINITY	REF
QPYLFATDSLK	Spherical Nanoparticles (Diameter = 4 nm)	TEM analysis indicated the presence of anatase and TiO ₂ (B)	1
GHTHYHAVRTQT	Spherical Nanoparticles (Diameter = 4 nm)	TEM analysis indicated the presence of anatase and TiO ₂ (B)	1
HKKPSKS	Interconnected network of spherical particles (≈50 nm)	Anatase Inclusions in the network	2
(LK)₈-PEG₇₀	Amorphous titania	Rutile phase induced after heating to 400°C	3
RKLPDAPGMHTW	Spherical nanoparticles (≈160 nm)	Anatase	4
SSKKS₂SGSYSGSKGSKRRIL	Interconnected network of spherical particles	No crystallinity reported	5
RKKRKKRKKRKKGGGY	Interconnected network of spherical particles	No crystallinity reported	5
Ac- MEELADSLEELARQVEELES A-CONH ₂	Interconnected network of spherical particles	No crystallinity reported	5
Ac- MKKLADS LKKLARQ VKKLESA -CONH ₂	Interconnected network of spherical particles	No crystallinity reported	5
Ac- MKQLADS LMQLARQ VSRLESA -CONH ₂	Interconnected network of spherical particles	No crystallinity reported	5
Ac- MKQLADS LHQLARQ VSRLEHA -CONH ₂	Interconnected network of spherical particles	No crystallinity reported	5
Ac- MKQLADS LHQLAHQ VSHLEHA -CONH ₂	Interconnected network of spherical particles	No crystallinity reported	5
Ac- PS ANSVAHS LANLAHS VSHLVSAD -CONH ₂	Interconnected network of spherical particles	No crystallinity reported	5
Ac- PS ANSVARS LANLARS VSRLVSAD CONH ₂	Interconnected network of spherical particles	No crystallinity reported	5
Ac- PS ANSVAKS LANLAKS VSKLVSAD -CONH ₂	Interconnected network of spherical particles	No crystallinity reported	5
SKSKKSKS	Spherical particles (≈500 nm)	No crystallinity reported	6

PROTEIN	PARTICLE MORPHOLOGY	CRYSTALLINITY	REF
Papain	Continuous film (Thickness \approx 100 nm)	Anatase inclusions (3-5 nm)	7
Silicatein	Spherical Nanoparticles (Diameter = 10 nm)	Lattice fringes observed in the TEM, but no crystallinity attributed to it	8
Sillafin	Spherical nanoparticles (5-40 nm)	Anatase crystallinity determined through SERS	9
Lysozyme	Spherical Nanoparticles (10-50 nm)	Amorphous	10
Protamine	Spherical nanoparticles (Diameter = 50 nm) with a fused morphology	Calcination at 600°C and 800°C for 2h induced anatase and rutile phase formation respectively	11
Catalase	Spherical Nanoparticles (< 5 nm)	Aging of samples between 3 to 4 weeks required to induce anatase	12
Lysozyme	Interconnected network of very fine particles (20-30 nm)	Aging of samples between 3 to 4 weeks required to induce mixed anatase and TiO ₂ (B)	12
Glucose Oxidase	Spherical Nanoparticles (3-5 nm)	Aging of samples between 3 to 4 weeks required to induce rutile	12

ORGANISM	PARTICLE MORPHOLOGY	CRYSTALLINITY	REF
Bacteriophage P22	Spherical Nanoparticles (Diameter \approx 10 nm)	Anatase	13

Table S2. Parameters used in COMSOL® simulations. (A) Parameters used to calculate the diffusion coefficient of sfGFP in 0.5% and 1.0% agarose hydrogels, and the Stokes-Einstein equation used for the calculation of the diffusion coefficient of sfGFP in an infinite solution. (B) Parameters and the Ogston Model equation used for the calculation of the diffusion coefficient of sfGFP in a hydrogel matrix. (C) The diffusion coefficient of copper nitriloacetate was used as a proxy for that of TiBALDH because both compounds have similar molecular masses (294.08 g mol⁻¹ for TiBALDH and 254 g mol⁻¹ for Cu-NTA).

A

Property	Symbol	Value	Unit
Dry Agarose Density	$\rho_{agarose}$	1.64	g ml ⁻¹
Mass Fraction of Agarose in a Fiber	$\omega_{agarose}$	0.625	
Concentration of Agarose	$C_{agarose}$	0.5	g ml ⁻¹
		1	g ml ⁻¹
Volume Fraction	$\phi_{0.5}$	$4.8 \cdot 10^{-3}$	
	ϕ_1	$9.7 \cdot 10^{-3}$	
Diffusion Coefficient in Hydrogel	$D_{0.5\%}$	$1.01 \cdot 10^{-10}$	m ² s ⁻¹
	$D_{1\%}$	$9.9 \cdot 10^{-11}$	m ² s ⁻¹
Porosity	$\Phi_{0.5\%}$	≈1	
	$\Phi_{1\%}$	≈1	

$$\text{Stokes-Einstein Equation } D_0 = \frac{k_B T}{6\pi\eta R_H}$$

B

Property	Symbol	Value	Unit
Boltzmann Constant	k_B	$1.38 \cdot 10^{-23}$	m ² kg s ⁻² K ⁻¹
Viscosity	η	$8.95 \cdot 10^{-4}$	kg m ⁻¹ s ⁻¹
Temperature	T	298	K
Hydrodynamic Diameter of sfGFP	R_H	$2.3 \cdot 10^{-9}$	m
Diffusion Coefficient in an infinite solution	D_0	$1.06 \cdot 10^{-10}$	m ² s ⁻¹

$$\text{Ogston Model } \frac{D_g}{D_0} = e^{-\phi^2 R_H / R_f}; \quad \phi = C_{agarose} / \rho_{agarose} \omega_{agarose}$$

C

Property	Value	Molecular Weight
Diffusion Coefficient of Copper nitriloacetate	$5 \cdot 10^{-10}$	254 g mol ⁻¹

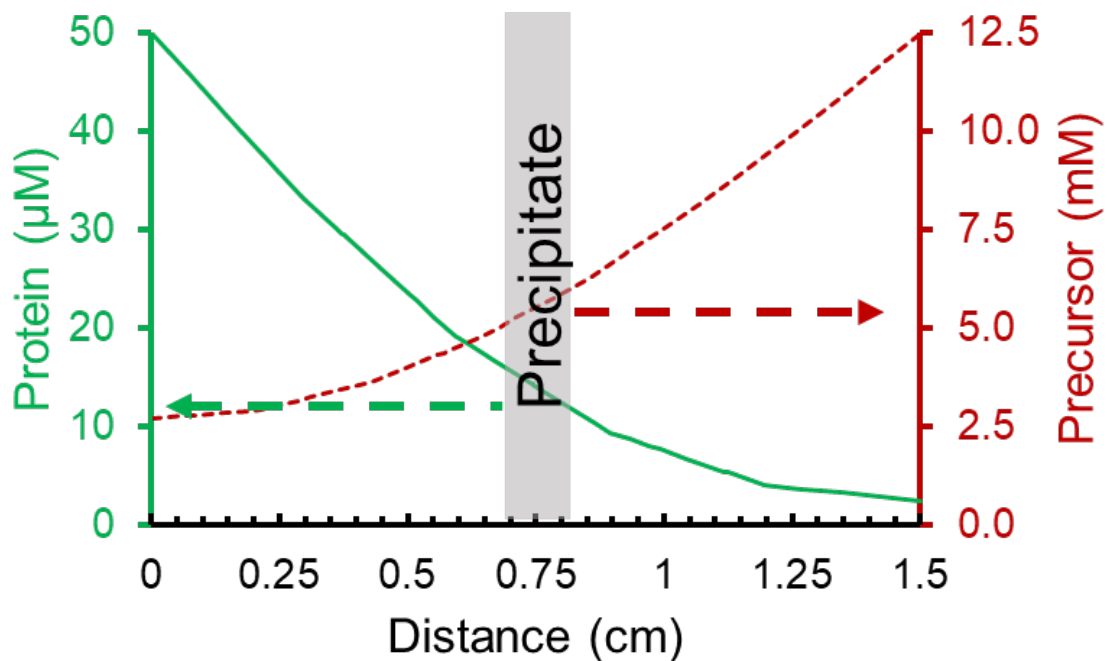


Figure S1. One-dimensional concentration profiles of protein and TiBALDH precursor in a 1.0% agarose hydrogel calculated using the transport of dilute species physics module of COMSOL® after a total diffusion time of 48h. Transport equations did not include a reaction component.

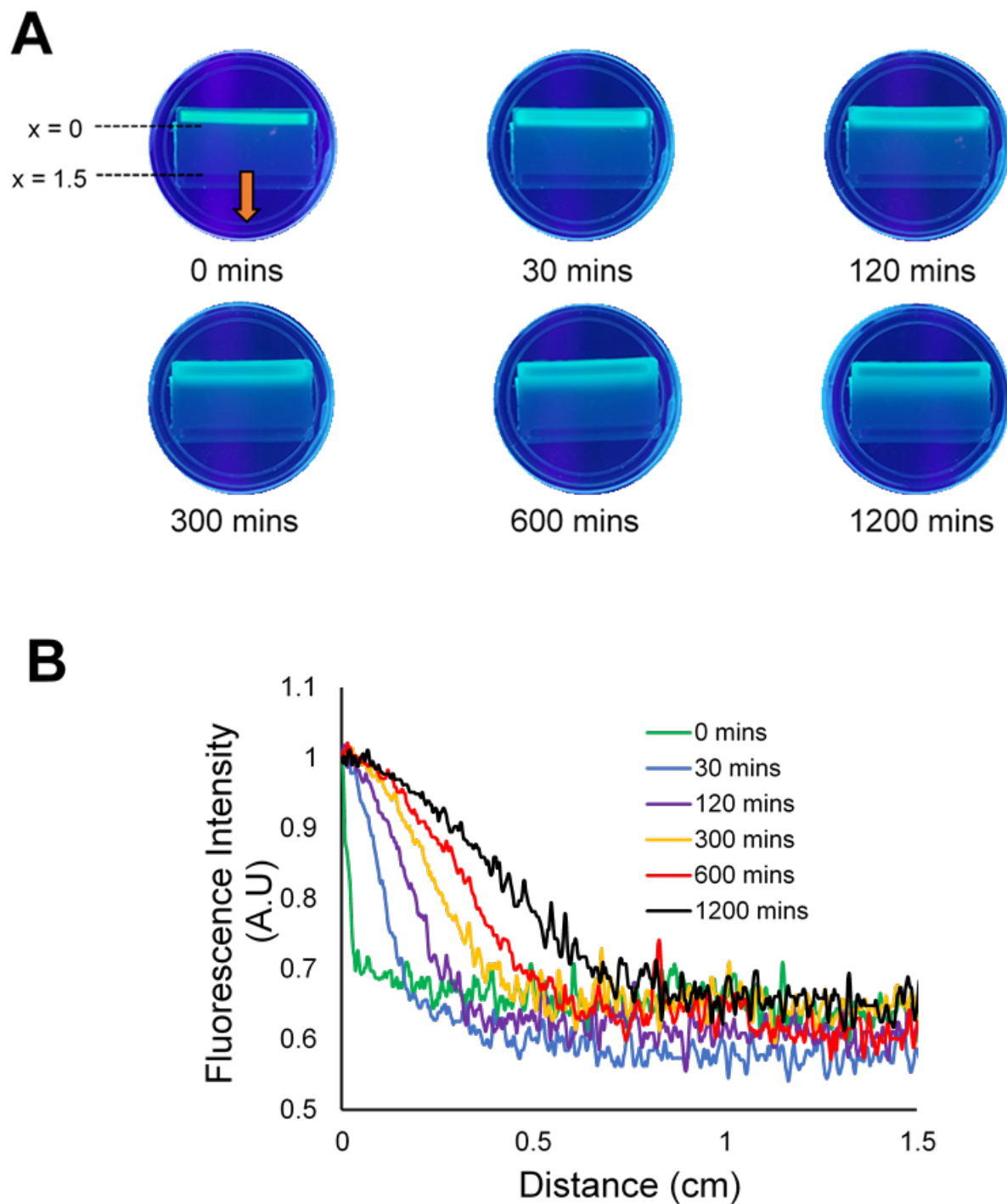


Figure S2. (A) Digital images of hydrogels illuminated with 365 nm UV light show protein diffusion at different time intervals. Labels $x = 0$ and $x = 1.5$ indicate the edges of the reactants loading wells and the orange arrow indicate the axis along which fluorescence intensity is quantified. (B) Digital images were converted to 8-bit images and the “Plot Profile” function of ImageJ was used to quantify pixel intensity as a function of distance. Intensities were normalized to the intensity value at $x = 0$ and plotted as a function of distance along the hydrogel at the indicated time intervals.

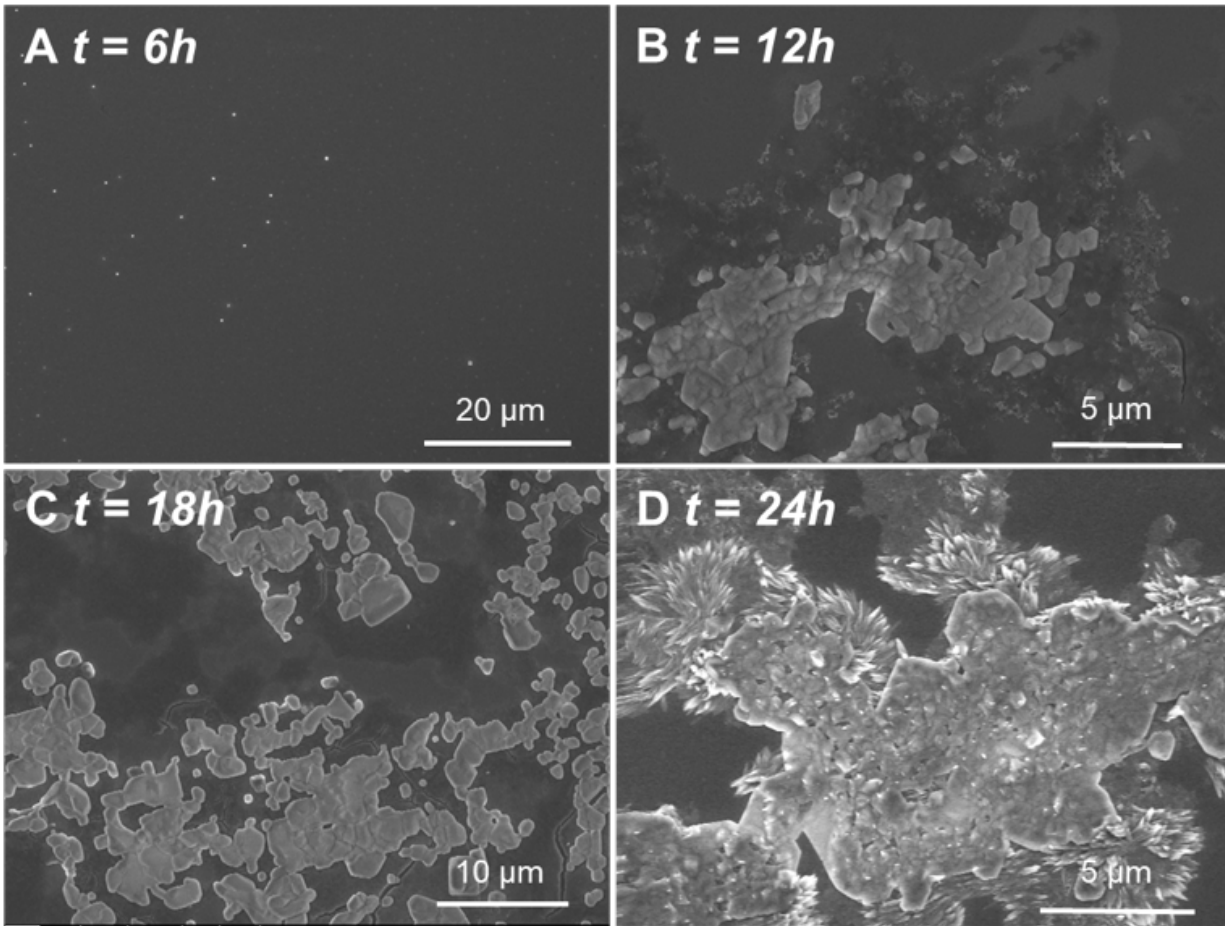


Fig S3. Evolution of the morphology of TiO₂ precipitated by sfGFP-Car9 at different reaction times in 0.5% agarose hydrogels. Representative scanning electron micrographs show the appearance of the precipitates at the indicated times.

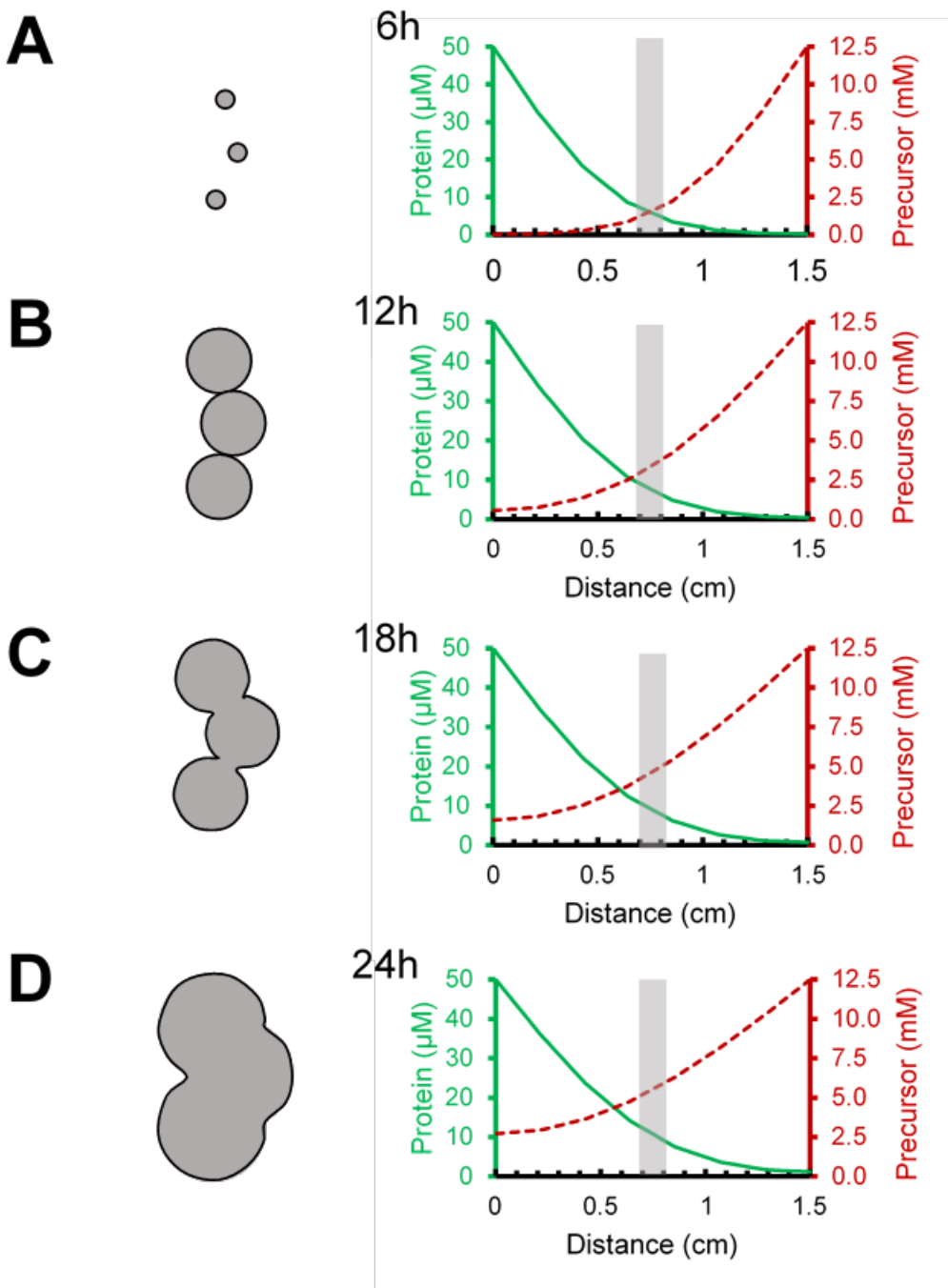


Figure S4. (Left) Cartoon representation of the evolution of the TiO₂ precipitate morphology over 24h of reaction. (Right) One-dimensional concentration profiles of protein and TiBALDH precursor in a 0.5% agarose hydrogel calculated using the transport of dilute species physics module of COMSOL® at the indicated reaction times. The grey bar indicates the region of interest which is excised for further analysis.

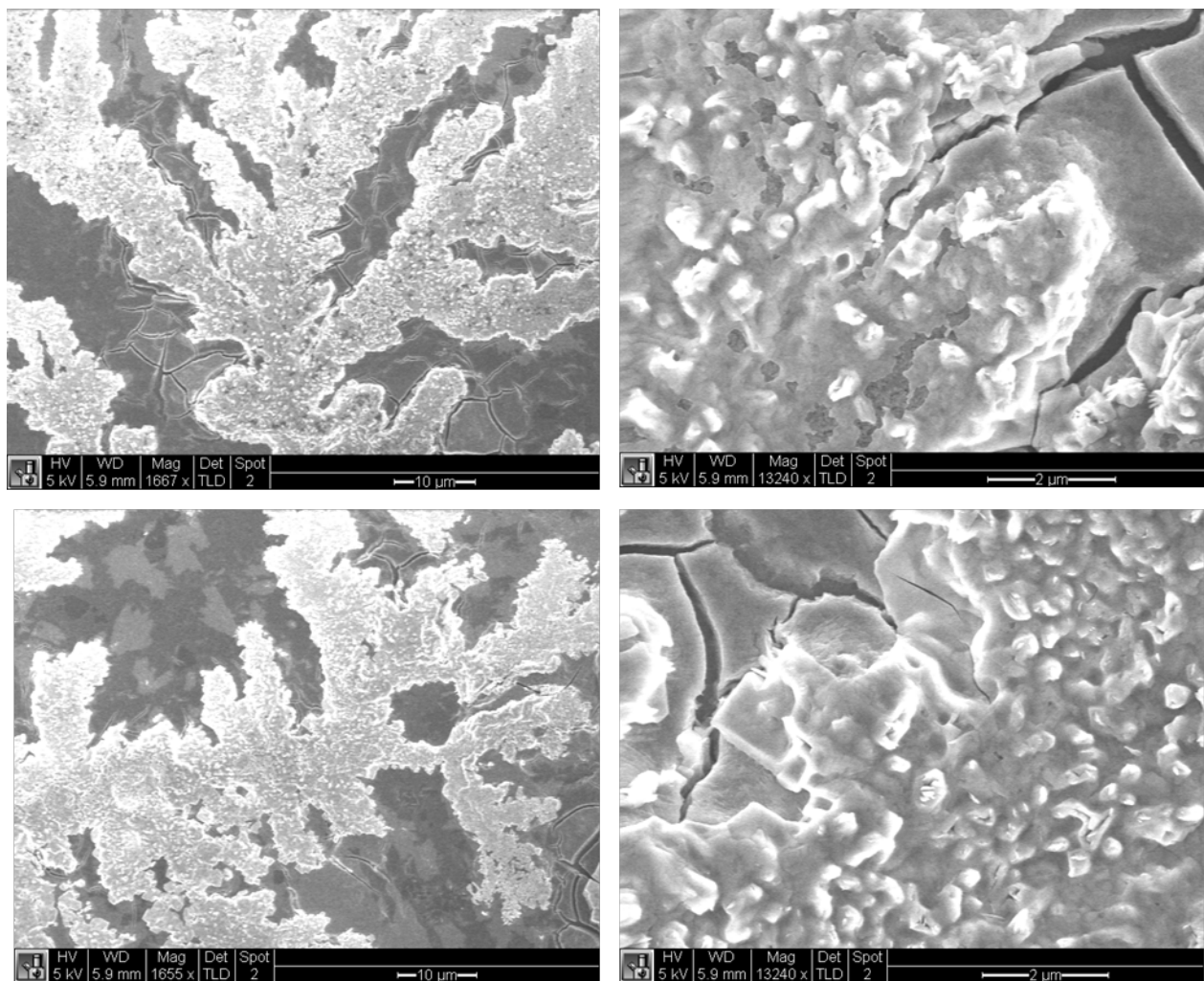


Figure S5. Representative SEM images showing titania precipitates obtained with sfGFP-Car9 after 2h of reaction in the absence of agarose hydrogel (bulk precipitation). Bulk precipitation of titania was conducted by mixing TIBALDH precursor (5 mM) and sfGFP-Car9 protein (10 μM) at concentrations obtained from COMSOL simulations in the reaction zone (grey region in Figure S4D).

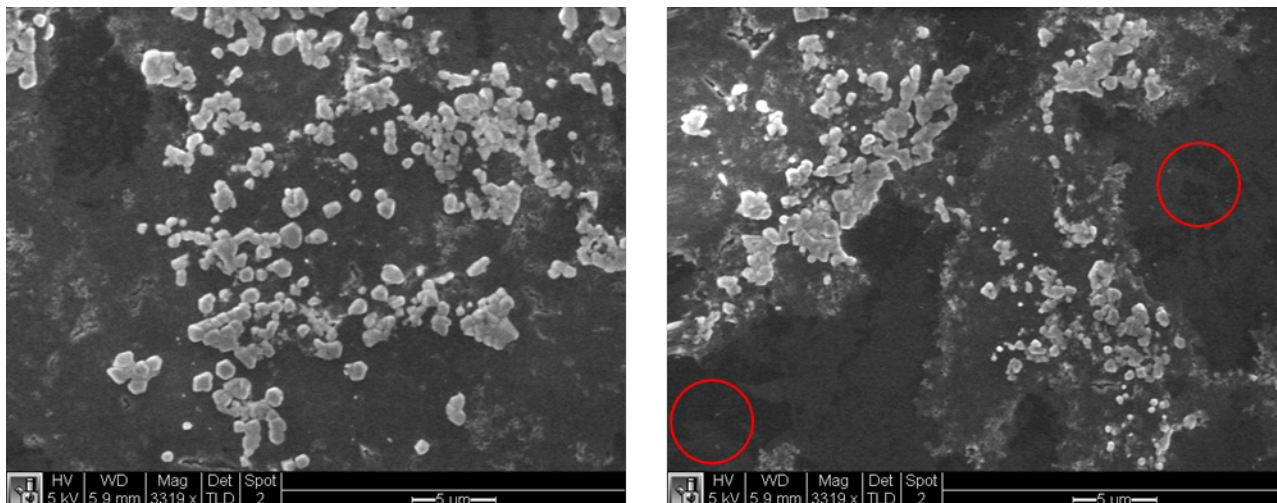


Figure S6. Representative SEM images of particles generated in the presence of sfGFP-Car9 in a 1.0% hydrogel after 24h reaction. Regions circled in red contain smaller nanoparticles (~200 nm in diameter).

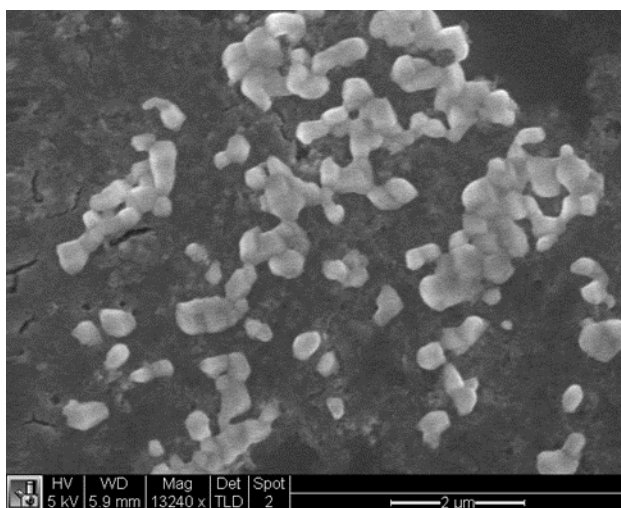
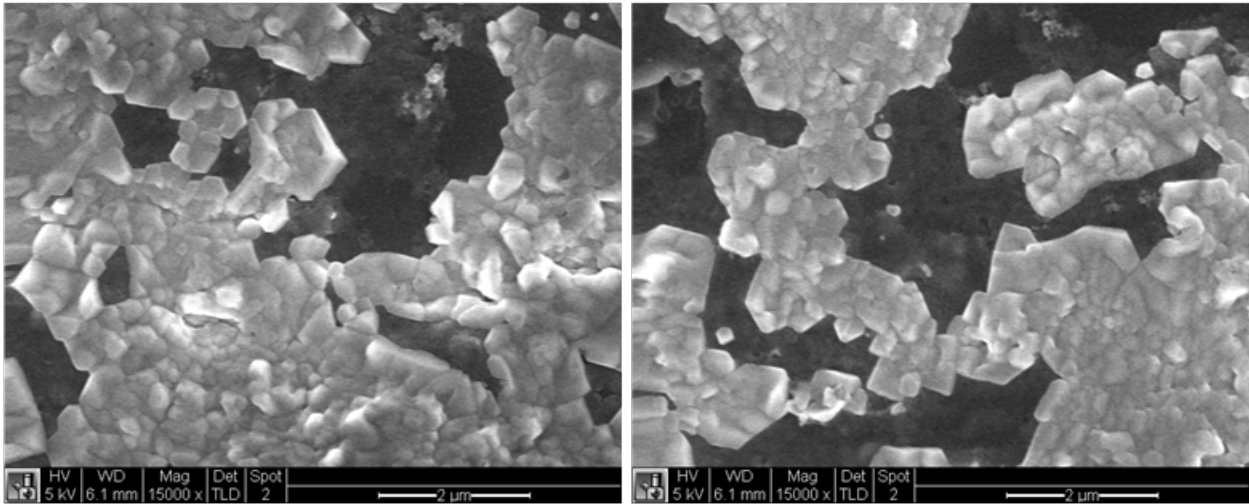
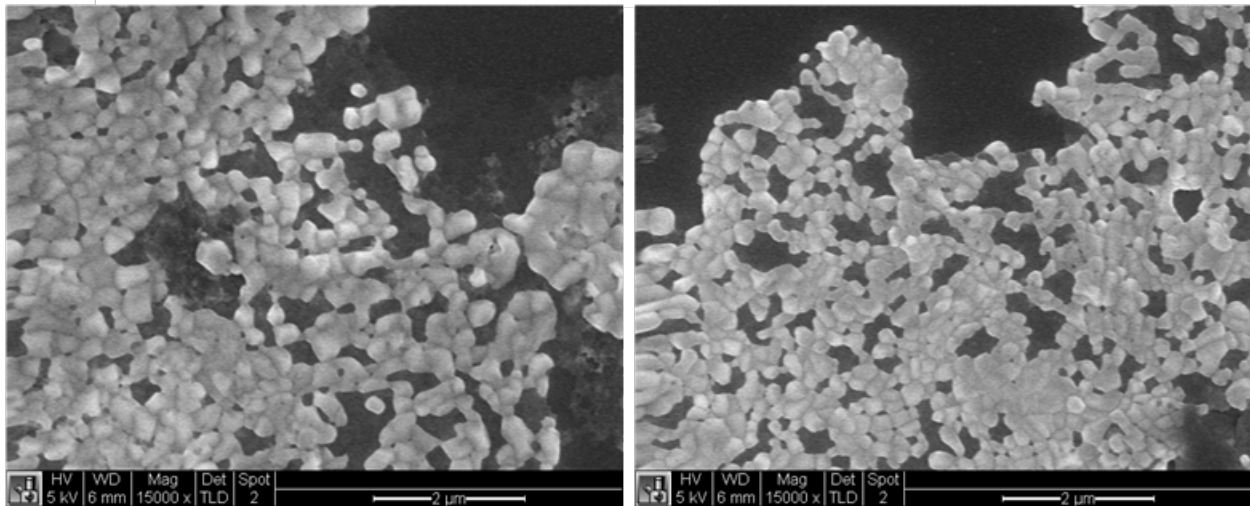


Figure S7. Representative SEM image of particles generated in the presence of mCherry-Car9 in a 1.0% hydrogel after 24h of reaction.

A MDSARGFKKPGKRGGGSENLYFQSMGRKGEEL...



B ...HNVEGSDSARGFKKPGKRTSDGSV...



C ...DELYKLGGS DSARGFKKPGKR

Figure S8. (A) Representative SEM images of titania precipitates obtained with Car9-sfGFP, a fusion protein in which the Car9 dodecapeptide (maroon) is followed by a flexible linker (purple), a TEV protease digestion site (red), and the mature sfGFP sequence (green).¹⁴ (B) Representative SEM images of titania precipitates obtained with sfGFP::Car9, a fusion protein in which the Car9 dodecapeptide is installed within permissive Loop 9 of sfGFP (green) with flanking GS/TS spacers (black).¹⁵ All reactions were conducted in a 1.0% hydrogel for 24h. (C) For comparison, the sequence for Car9 installed at the C-terminus of sfGFP is shown: the C-terminal sfGFP sequence (green) is followed by a flexible linker (purple) and terminated by the Car9 sequence (maroon).

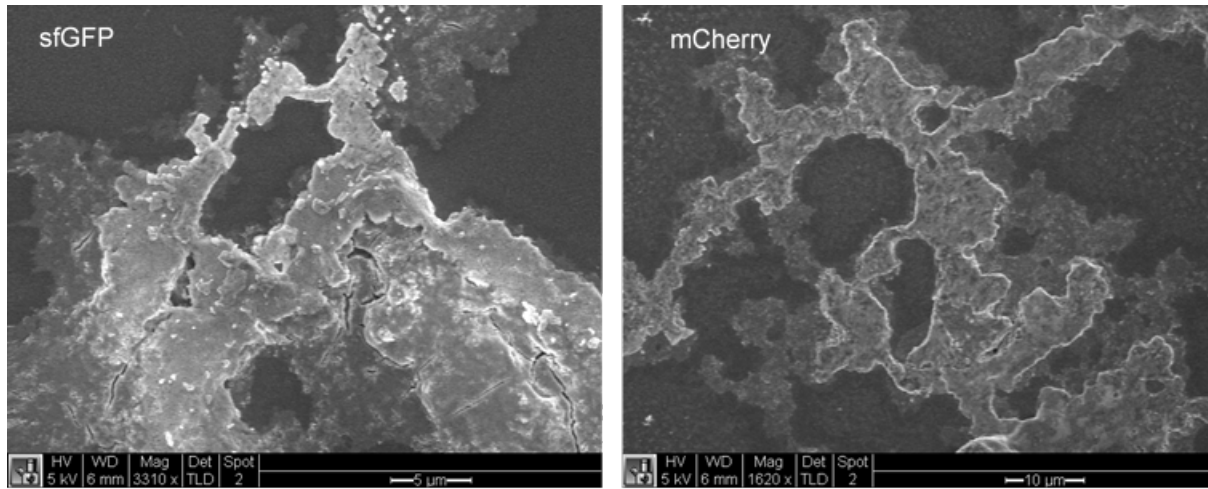


Figure S9. Representative SEM images showing titania precipitates obtained with wild type sfGFP (left) and wild type mCherry (right) in 1.0% agarose hydrogels after 24h of reaction.

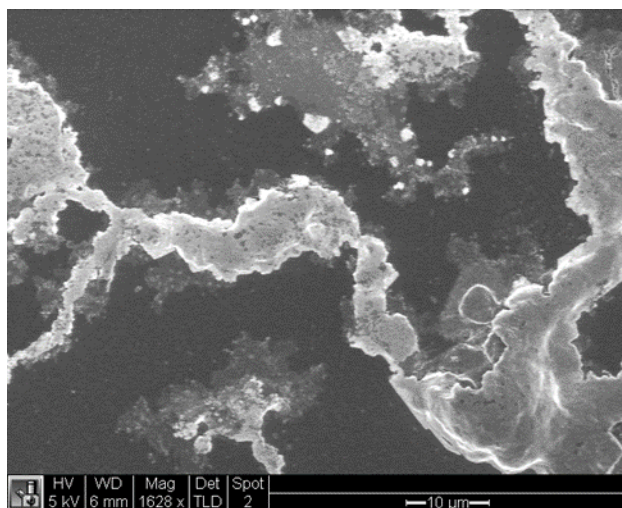


Figure S10. Representative SEM image of a titania precipitate obtained with sfGFP-Car9 in a 1.0% agarose hydrogel after 48h of reaction.

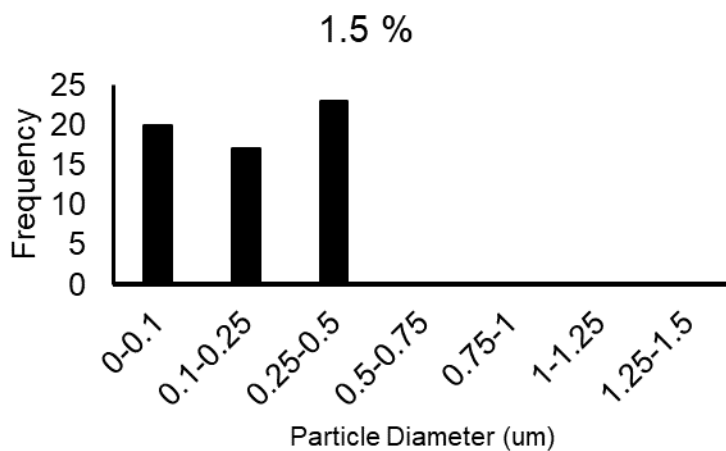
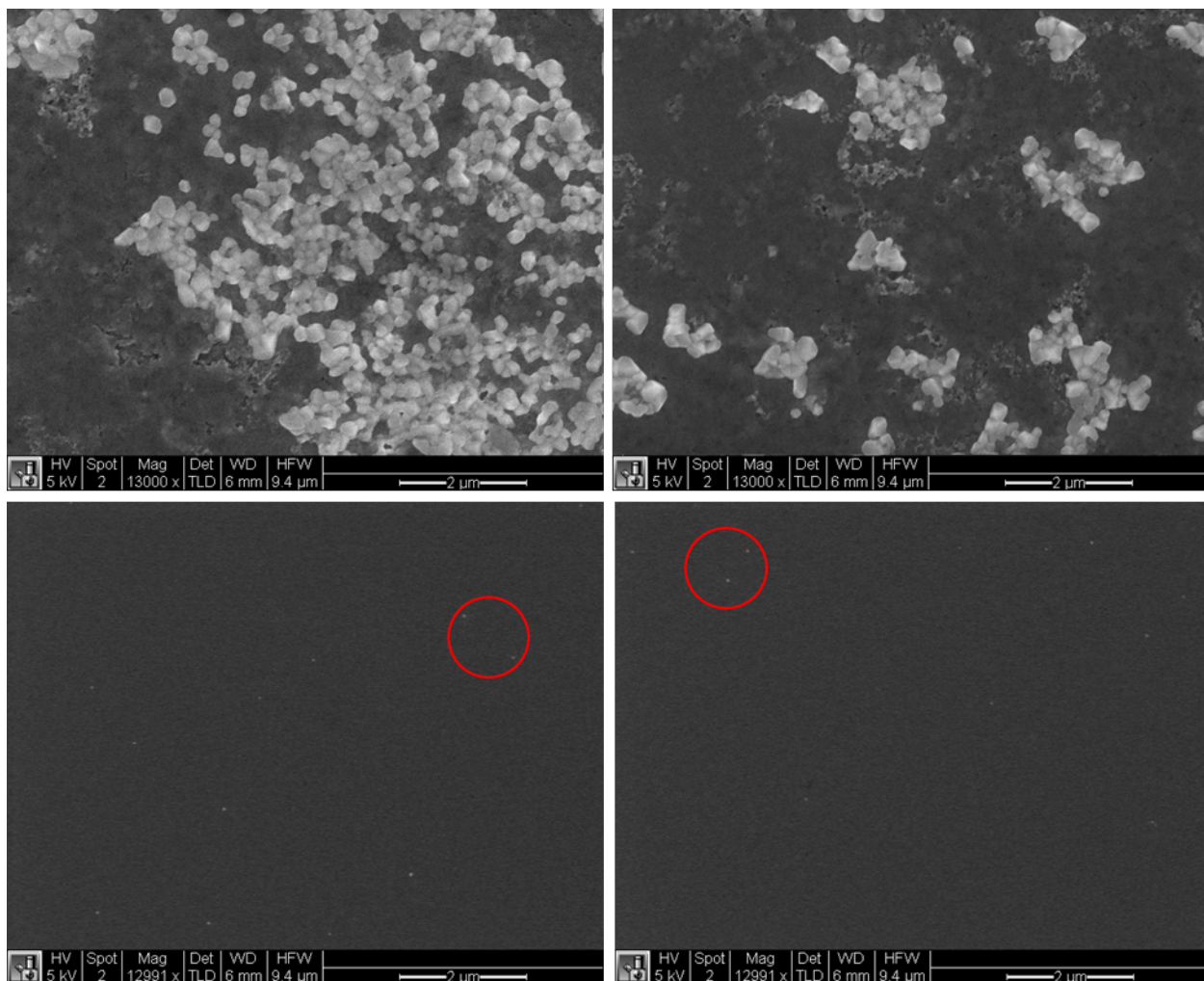


Figure S11. Representative SEM images of TiO₂ particles obtained with sfGFP-Car9 in a 1.5% agarose hydrogel after 24h of reaction. The lower SEMs show a subpopulation of smaller particles. Histograms show the size distribution of n = 60 particles measured with Image J.

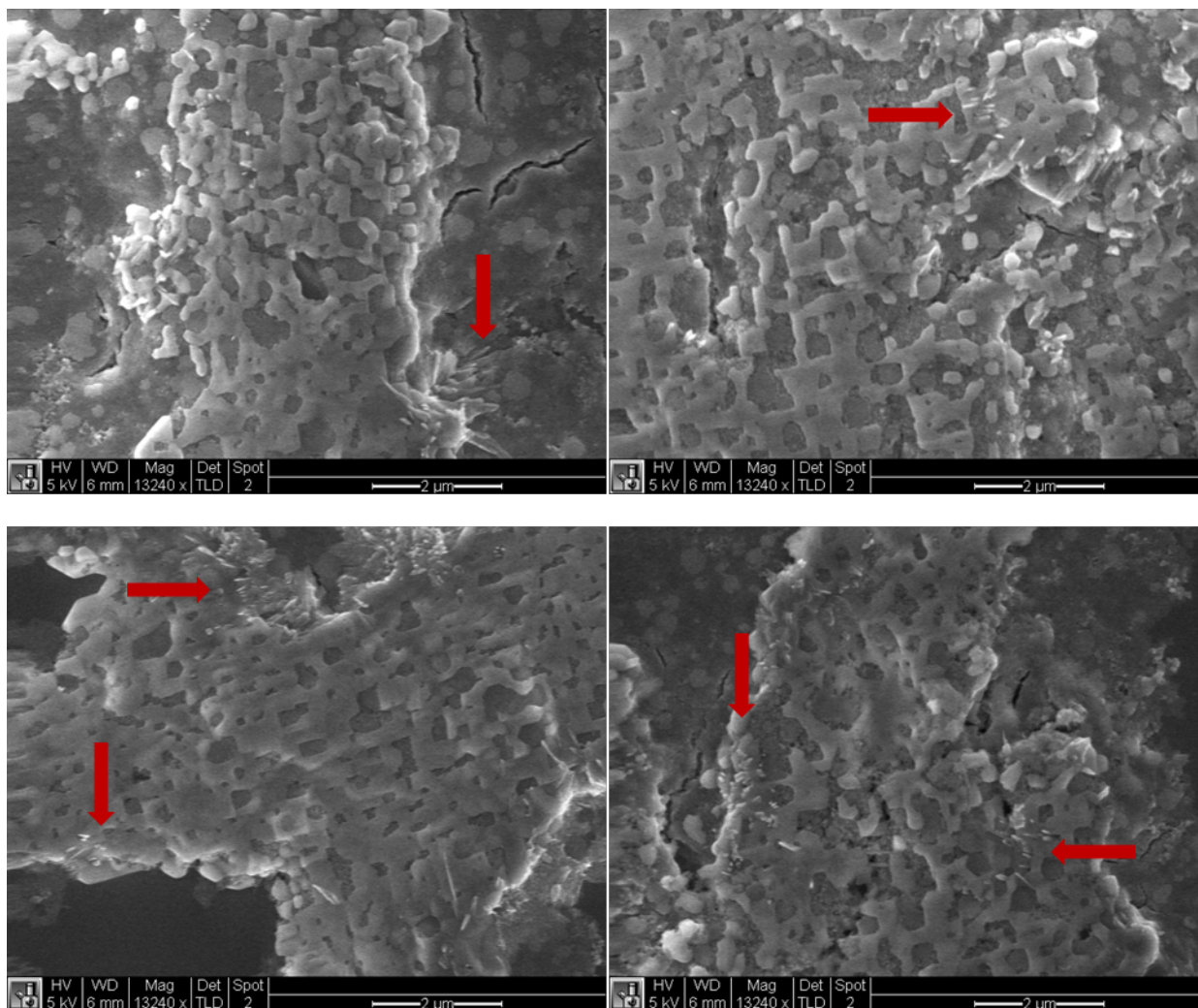


Figure S12. Representative SEM images of a bridged TiO₂ network obtained with sfGFP-Car9 in a 0.75% agarose hydrogel after 24h of reaction. The red arrows identify needles that are found in abundance in samples prepared in 0.5% agarose hydrogels.

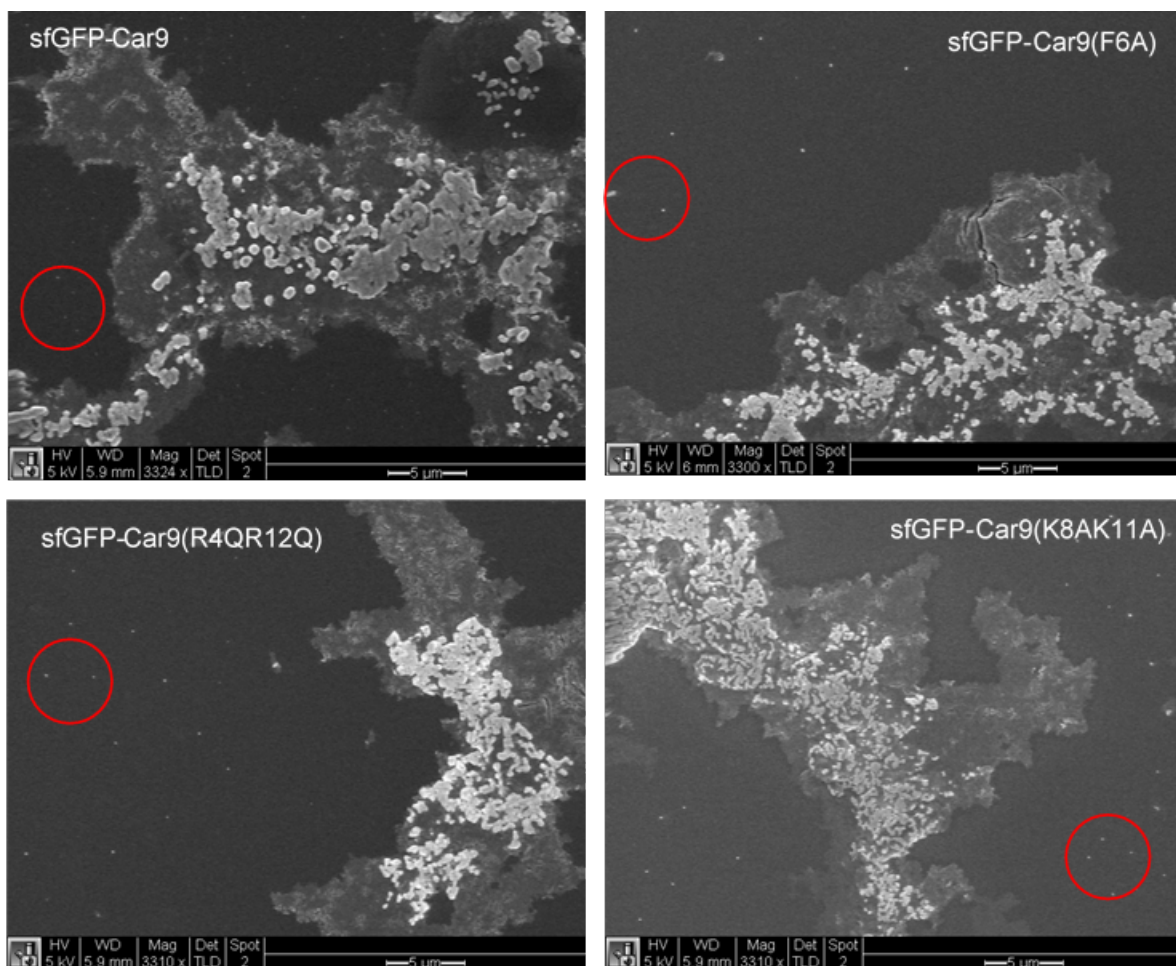


Figure S13. Representative scanning electron micrographs of spheroidal particles generated in the presence of sfGFP-Car9 and the indicated mutants in a 1.0% agarose hydrogel after 24h of reaction. Regions circled in red contain smaller nanoparticles ≈ 200 nm is diameter.

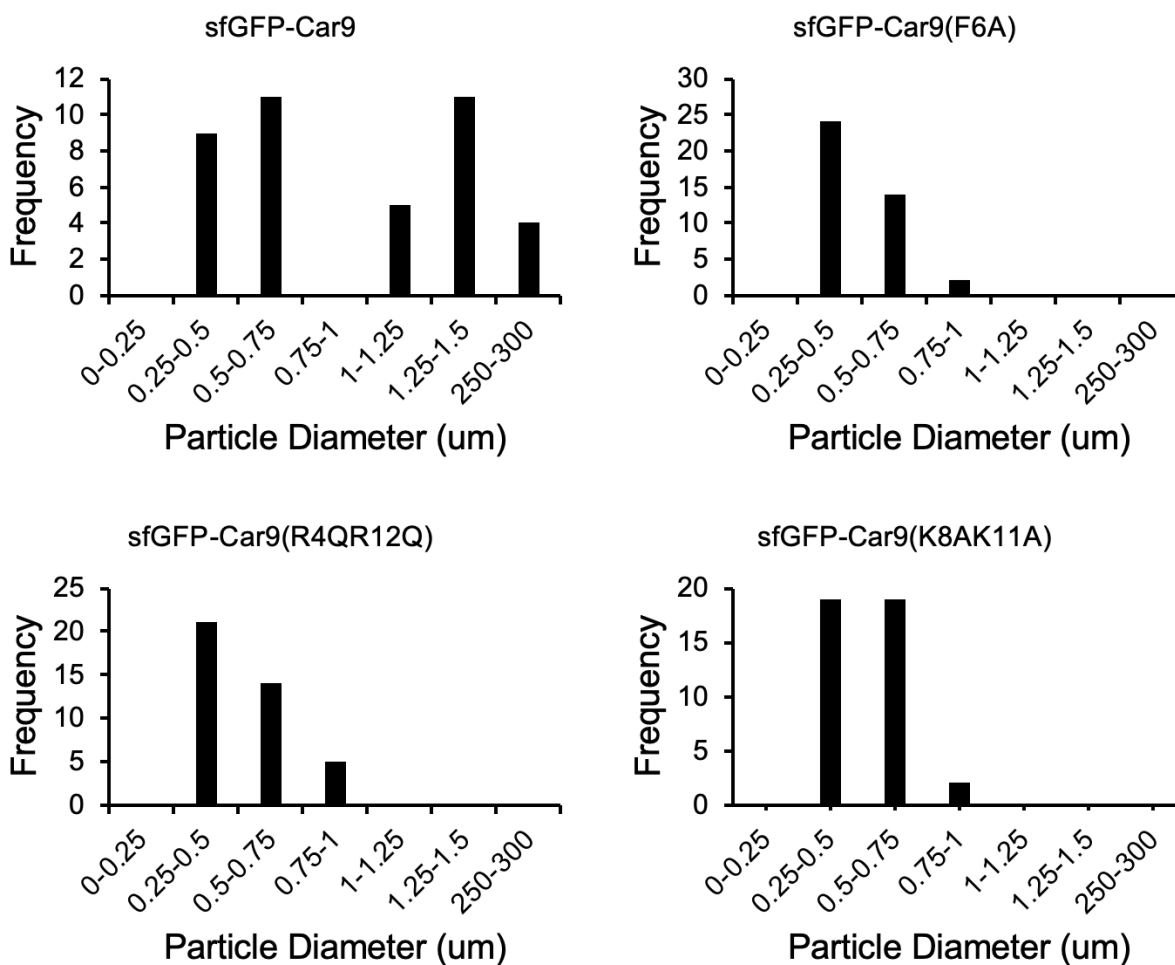


Figure S14. Histograms showing the size distribution of particles precipitated by sfGFP-Car9 and the indicated mutants after 24h of reaction in 1.0% agarose hydrogels. Particle sizes (n = 40) were measured using ImageJ.

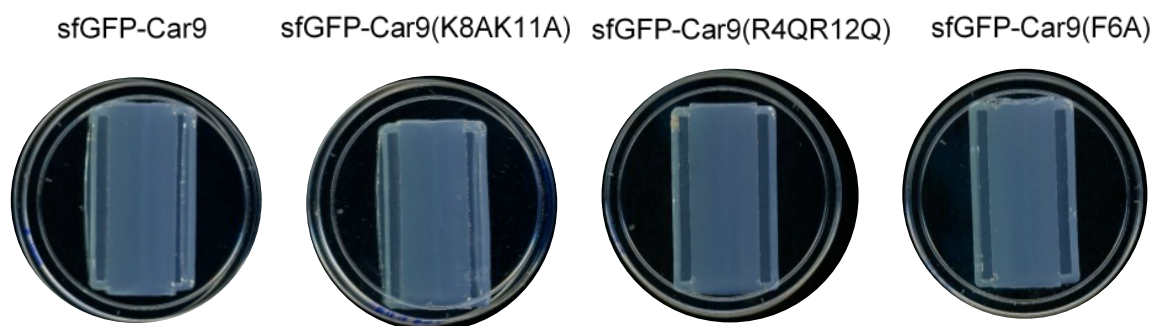
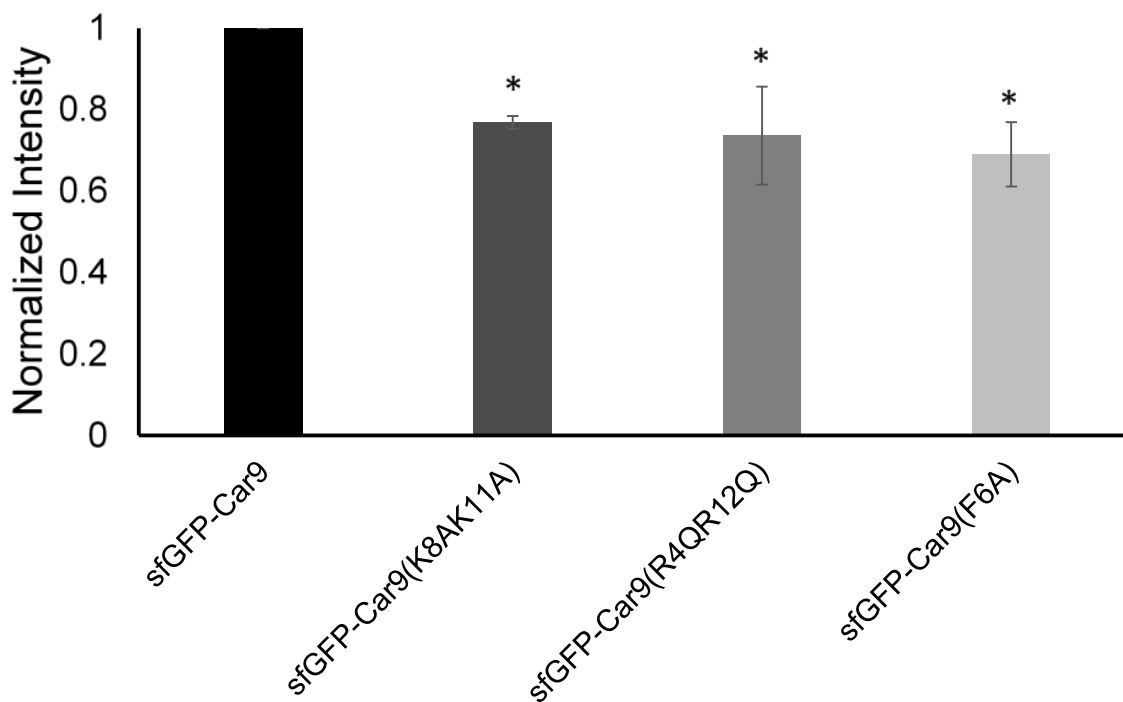
A**B**

Figure S15. (A) Digital Images of precipitates obtained after 24h of reaction in 1.0 % agarose hydrogels with the indicated proteins. (B) The intensities of the precipitates bands, observable as white lines in the centerlines of the gels, were quantified using ImageJ to estimate precipitate yields. Briefly, images were converted to 8-bit and the maximum threshold value manually set to 100. Band intensities were acquired by subtracting the threshold value at which the white bands appear and the threshold value at which they disappear through manual balancing of the minimum threshold slider. Intensities were normalized to that of the precipitate obtained with sfGFP-Car9. Stars indicate statistical relevance (two-way t test with $p < 0.05$). Results are highly consistent with the precipitation yields obtained with the same proteins under bulk precipitation conditions (Langmuir, 2020, 36:8503-10).

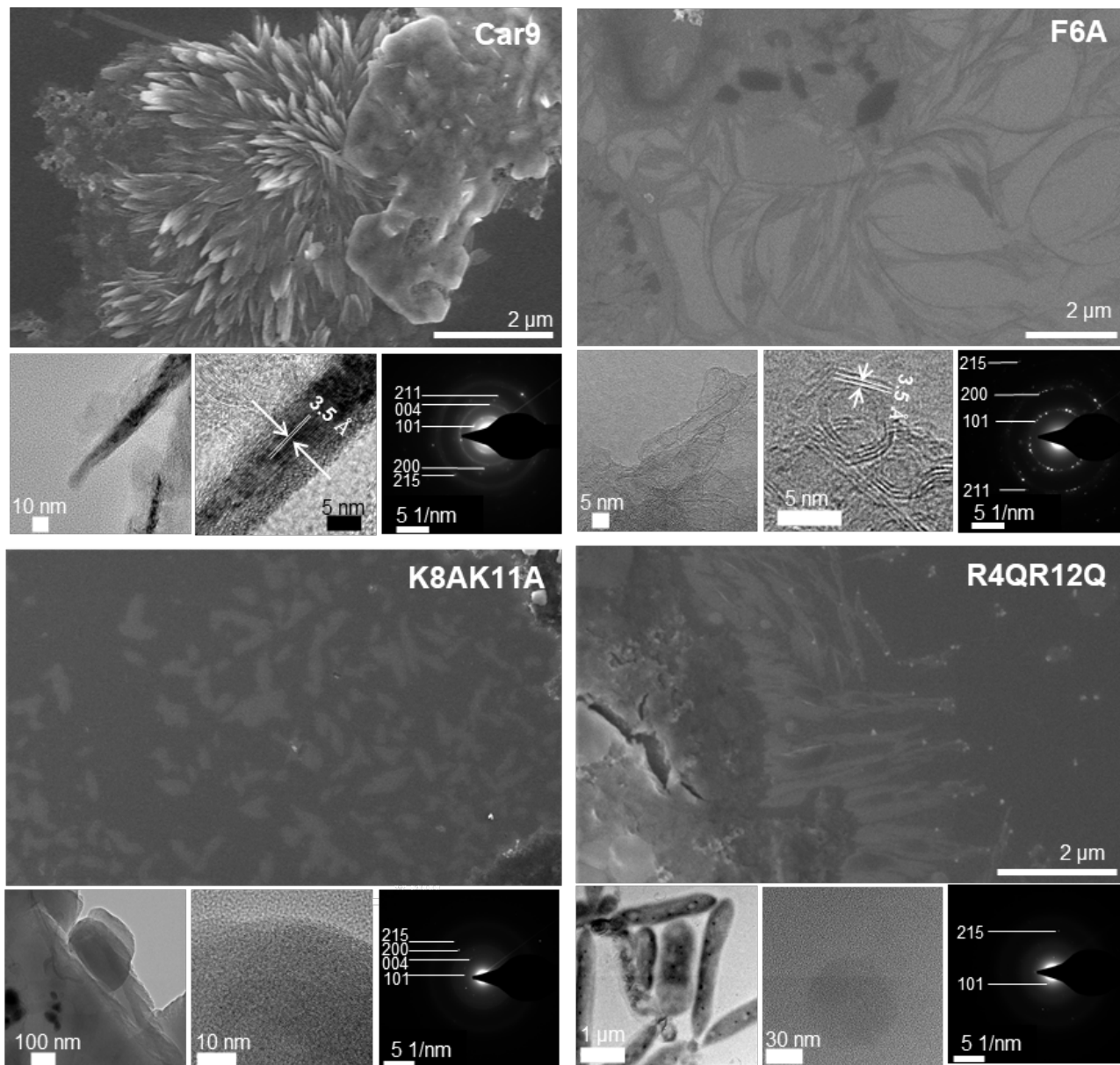


Figure S16. Enlarged image of Fig. 3. SEM (top panels) and TEM (bottom panels) characterization of titania precipitates obtained using (A) wild type sfGFP-Car9, (B) sfGFP-Car9(F6A), (C) sfGFP-Car9(K8AK11A), and (D) sfGFP-Car9(R4QR12Q) as the protein inducer. All experiments were conducted in a RDC operated with a 0.5% agarose gel. Samples were excised after 24h of reaction. TEM imaging was conducted at low (bottom left) and high resolution (bottom center). Selected area diffraction (SAED) patterns (bottom right) were acquired on the high-resolution fields shown and are indexed to anatase titania.

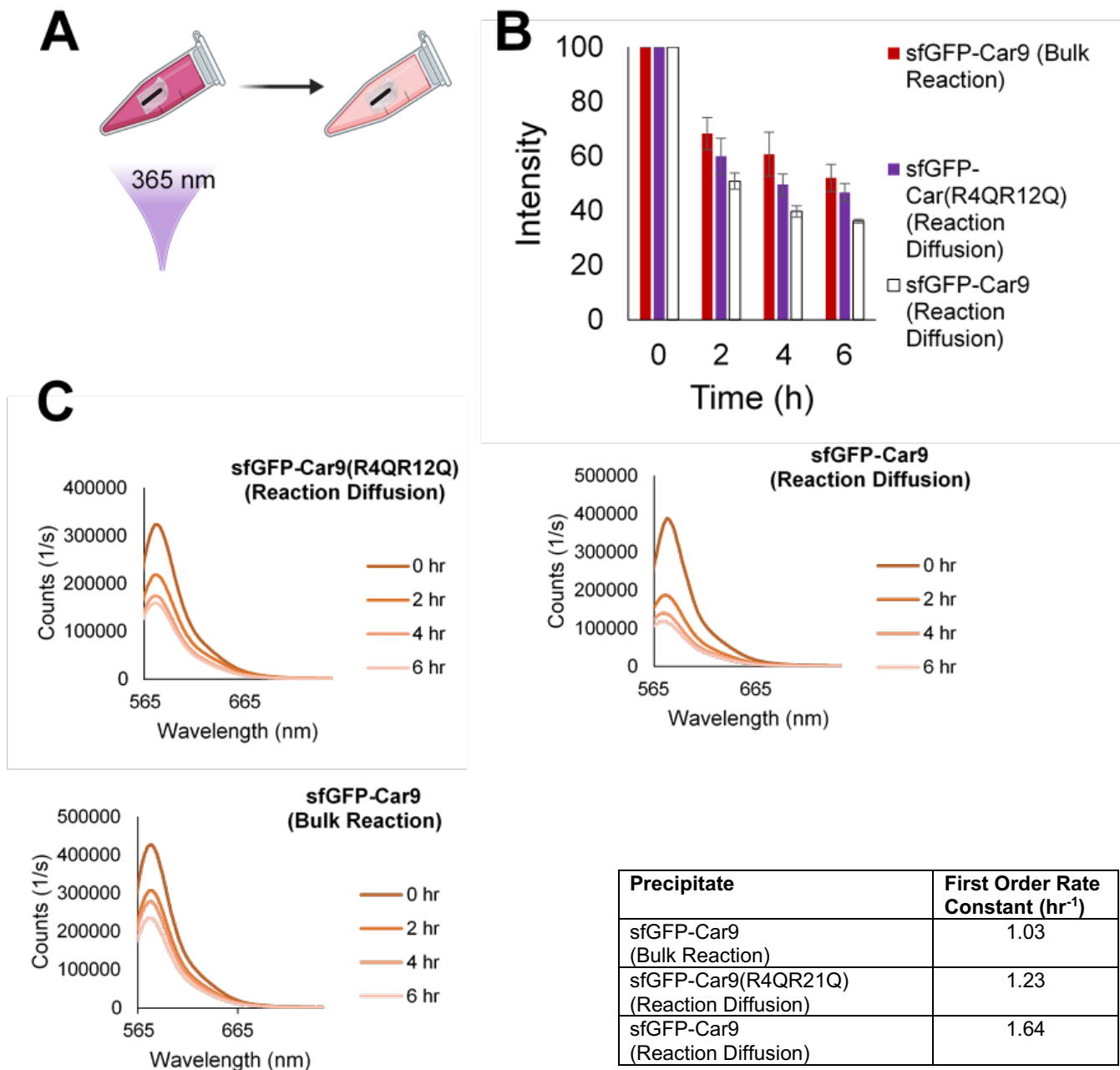


Figure S17. (A) Cartoon representation of the experimental setup for demonstration of photocatalytic activity of bio-precipitated titania through photodegradation of Rhodamine B, (B) Graph indicating the decrease of fluorescence intensity normalized to the fluorescence intensity at $t=0$ as a function of time (0, 2, 4 and 6 hr) and (C) Fluorescence spectra of as a function of time (0, 2, 4 and 6 hr) for the precipitates employed along with their calculated first order rate constant. Bulk precipitant of titania is generated from the concentrations obtained from COMSOL simulations in the reaction zone (grey region in Figure S2D) of precursor (5 mM) and sfGFP-Car9 (10 μM).

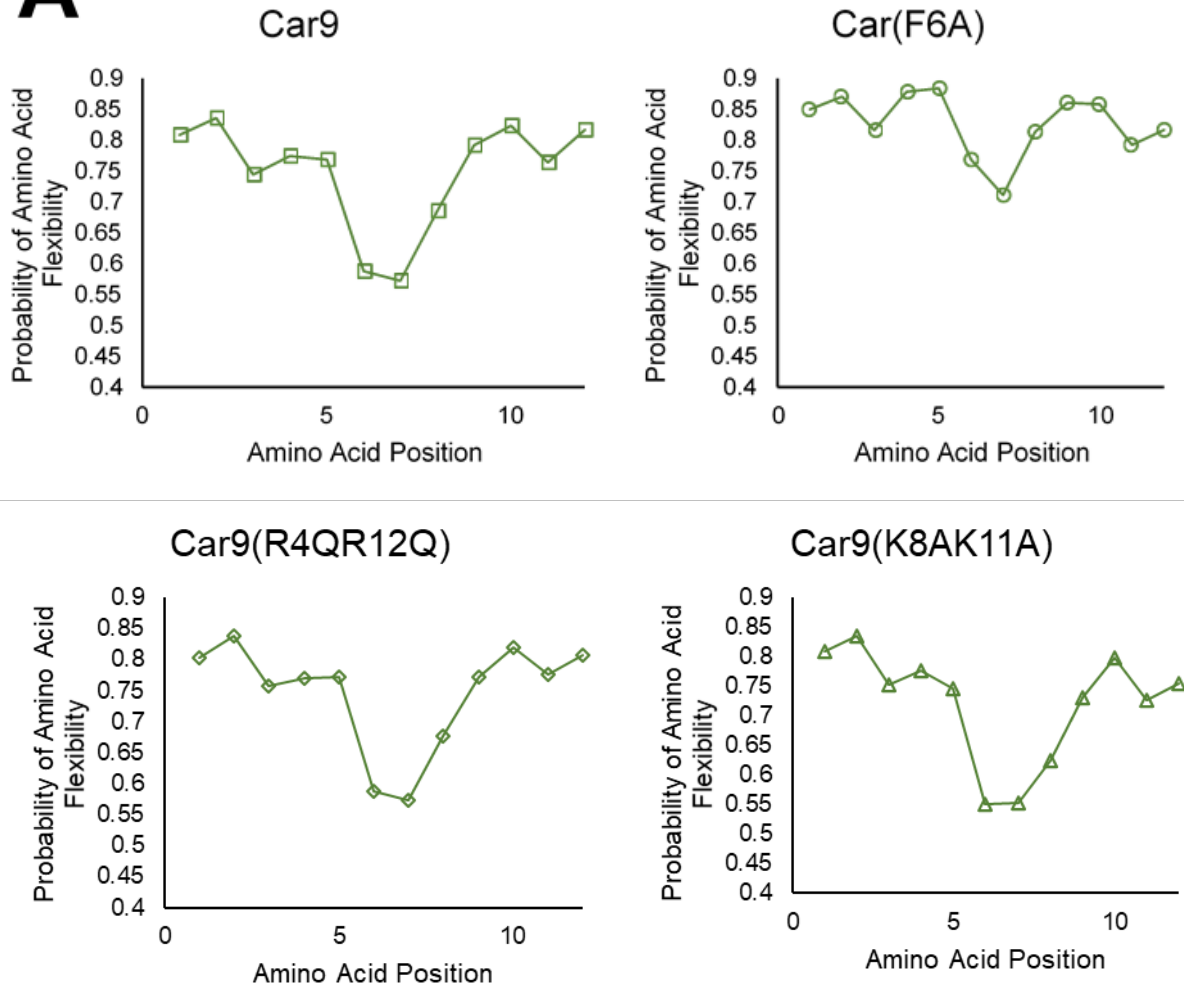
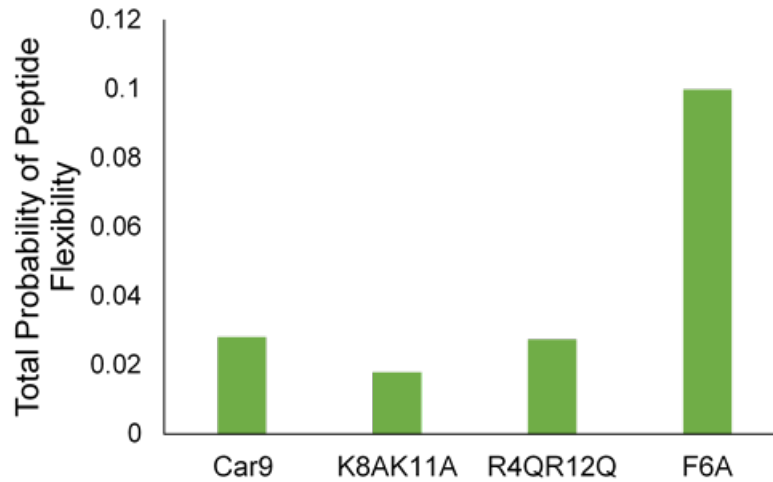
A**B**

Figure S18. (A) Predicted flexibility of amino acids along the sequences of the Car9 and its mutants using the FlexPred webserver.¹⁶ (B) Total peptide flexibility calculated as the product of individual amino acid residue probabilities.

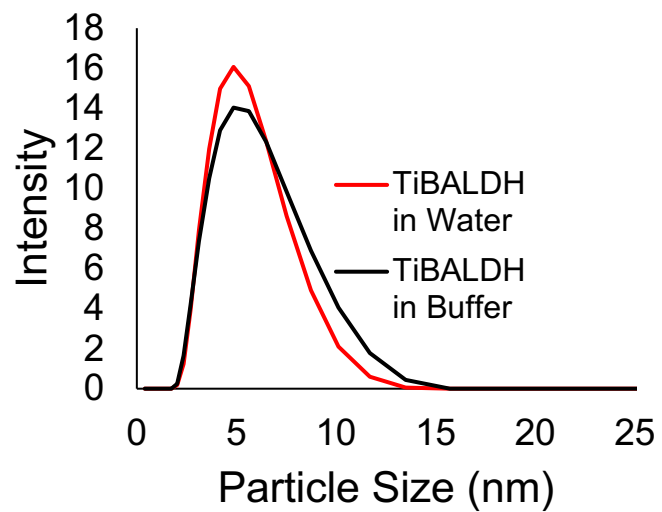


Figure S19. Dynamic light scattering measurements show the presence of 2-5 nm titania nanoparticles in 12.5 mM TiBALDH stock solutions prepared in water and in sodium citrate buffer at pH 5.

Experimental Section

Materials

TIBALDH (described as Titanium(IV) bis(ammonium lactato)dihydroxide but formulated as $(\text{NH}_4)_2\text{Ti}_2\text{O}_4(\text{Lactate})_8 \cdot 4\text{H}_2\text{O}$) was purchased from Sigma-Aldrich. UltraPure™ agarose was purchased from Invitrogen. All chemicals were used as received from the manufacturer. MilliQ water at a resistivity of 18.2 MΩ cm was used as a solvent for all experiments.

Methods

Protein Purification. Wild type sfGFP, sfGFP-Car9, and sfGFP-Car9 variants containing the F6A, R4QR12Q and K8AK11A mutations in their Car9 segment were expressed and purified as described.^{2, 3}

Reaction Diffusion Chamber (RDC) Construction and TiO₂ Precipitation Reactions. The chamber depicted in **Figure 1B** was built through machining and polishing acrylic pieces from a larger rectangular piece into the desired dimension (5 cm x 2.5 cm x 7 mm). Parts were bonded together using an acrylic glue. The final dimension of the combs employed to create the reagent reservoirs are 4 cm (Length) x 6 mm (Height) and 4 mm (Thickness). In a typical experiment, agarose at the indicated weight to volume percentage (0.5, 0.75 or 1.0%) is added to a 37.5 mM sodium citrate buffer held at pH 5. The mixture is heated in a conventional microwave for 30 seconds in 10 second intervals to completely dissolve the agarose. The resulting clear solution (5 mL) is poured into the chamber fitted with the two flanking combs. The gel is allowed to solidify for 30 minutes at room temperature and the combs are carefully removed to create reagent wells. The gel along with the chamber are then transferred to a 150 mm x 15 mm Petri dish and 300 μL of the indicated protein is added at 50 μM concentration in one of the wells. About 3 ml of water is added to the bottom of the dish to prevent dehydration. A lid is placed on the dish and protein diffusion is allowed to proceed for 24h. At the end of that period, 300 μL of 12.5 mM TiBALDH in 37.5 mM sodium citrate buffer, pH 5.0 is added to the second well and the precursor is allowed to diffuse 24 or 48h.

Sample Preparation. Precipitated products are removed by excision of a 5 mm x 4 cm x 7.5 mm region of the gel at the indicated time points using a razor blade. The gel slice (approximate volume 100 μL) is mixed with 700 μL of 94% bleach in a 1.5 ml Eppendorf tube and immersed in a water bath held at 65°C for 30 min to dissolve the agarose and remove surface-bound proteins. Samples are centrifuged at 8,000g for 5 minutes, and washed twice by addition of 1 mL bleach solution and centrifugation at 8,000g for 5 minutes. Finally, samples are washed three times with 1 mL of MilliQ water to remove any remaining bleach and resuspended through pipetting in 100 μL of MilliQ water.

Electron Microscopy. For SEM experiments, aliquots (3 μL) of the various samples were deposited on a silicon wafer and images were acquired on a FEI Sirion XL30 operated at 5 kV and a spot size of 2 using the instrument's ultrahigh resolution mode. From TEM images, sample aliquots (10 μL) were deposited on a C-flat holey carbon grid and excess solution was wicked with a filter paper. Images were collected on a FEI Tecnai G2 SuperTwin operating at an acceleration voltage of 200 kV. Selected area electron diffraction patterns were acquired in the TEM.

Photodegradation of Rhodamine. Excised hydrogel bands containing the precipitates are placed in 10 ml water for 2 days to remove unreacted proteins/precursor. The hydrogel slice is then placed in an Eppendorf tube containing 2 ml of 1 μM rhodamine B. The tube is irradiated at 365 nm using a UV-transilluminator. The fluorescence intensity of rhodamine B is measured at time intervals of 0, 2, 4 and 6 hours through a fluorescence spectrophotometer with an excitation wavelength of 546 nm and an emission scan from 565 nm to 750 nm.

1. V. Puddu, J. M. Slocik, R. R. Naik and C. C. Perry, *Langmuir*, 2013, **29**, 9464-9472.
2. A. Hernández-Gordillo, A. Hernández-Arana, A. Campero and L. I. Vera-Robles, *Langmuir*, 2014, **30**, 4084-4093.
3. T. Nonoyama, T. Kinoshita, M. Higuchi, K. Nagata, M. Tanaka, K. Sato and K. Kato, *J. Am. Chem. Soc.*, 2012, **134**, 8841-8847.
4. A. P. Schoen, D. T. Schoen, K. N. L. Huggins, M. A. Arunagirinathan and S. C. Heilshorn, *J. Am. Chem. Soc.*, 2011, **133**, 18202-18207.
5. C.-X. Zhao, L. Yu and A. P. J. Middelberg, *RSC Adv.*, 2012, **2**, 1292-1295.
6. E. L. Buckle, J. S. Lum, A. M. Roehrich, R. E. Stote, B. Vandermoon, M. Dracinsky, S. F. Filocamo and G. P. Drobny, *J. Phys. Chem. B*, 2018, **122**, 4708-4718.
7. L. A. Bawazer, J. Ihli, M. A. Levenstein, L. J. C. Jeuken, F. C. Meldrum and D. G. G. McMillan, *J Mater Chem B*, 2018, **6**, 3979-3988.
8. L. A. Bawazer, M. Izumi, D. Kolodin, J. R. Neilson, B. Schwenzer and D. E. Morse, *Proceedings of the National Academy of Sciences*, 2012, **109**, E1705.
9. E. Kharlampieva, C. M. Jung, V. Kozlovskaya and V. V. Tsukruk, *J. Mater. Chem.*, 2010, **20**, 5242-5250.
10. H. R. Luckarift, M. B. Dickerson, K. H. Sandhage and J. C. Spain, *Small*, 2006, **2**, 640-643.
11. Y. Jiang, D. Yang, L. Zhang, L. Li, Q. Sun, Y. Zhang, J. Li and Z. Jiang, *DTr*, 2008, 4165-4171.
12. G. Chen, M. Li, F. Li, S. Sun and D. Xia, *Adv. Mater.*, 2010, **22**, 1258-1262.
13. G. J. Bedwell, Z. Zhou, M. Uchida, T. Douglas, A. Gupta and P. E. Prevelige, *Biomacromolecules*, 2015, **16**, 214-218.
14. J. Soto-Rodríguez, B. L. Coyle, A. Samuelson, K. Aravagiri and F. Baneyx, *Protein Expr. Purif.*, 2017, **135**, 70-77.
15. B. J. F. Swift, J. A. Shadish, C. A. DeForest and F. Baneyx, *J. Am. Chem. Soc.*, 2017, **139**, 3958-3961.
16. I. B. Kuznetsov and M. McDuffie, *Bioinformatics*, 2008, **3**, 134-136.